

See discussions, stats, and author profiles for this publication at: <https://www.researchgate.net/publication/295678415>

Functionalization of 4-aminothiophenol and 3-aminopropyltriethoxysilane with graphene oxide for potential dye and copper removal

Article in *Journal of hazardous materials* · February 2016

DOI: 10.1016/j.jhazmat.2016.02.040

CITATION

1

READS

39

4 authors, including:



[Hongyu Wang](#)

Wuhan University

53 PUBLICATIONS 73 CITATIONS

SEE PROFILE



Functionalization of 4-aminothiophenol and 3-aminopropyltriethoxysilane with graphene oxide for potential dye and copper removal



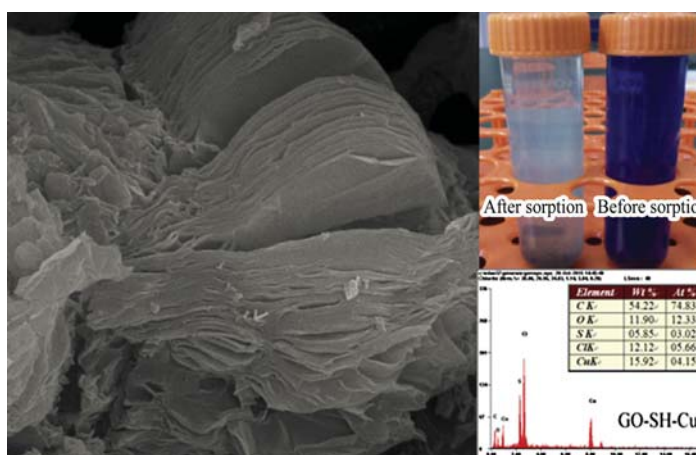
Dan Chen¹, Huining Zhang¹, Kai Yang, Hongyu Wang*

School of Civil Engineering, Wuhan University, Wuhan 430072, China

HIGHLIGHTS

- Two novel engineered GO were used to remove MB and Cu²⁺ from aqueous solutions.
- Characterization tests showed that –SH and –NH₂ were existed onto GO-SH and GO-N.
- This modification on GO improved the sorption capacities of MB and Cu²⁺.

GRAPHICAL ABSTRACT



ARTICLE INFO

Article history:

Received 25 December 2015
 Received in revised form 12 February 2016
 Accepted 19 February 2016
 Available online 22 February 2016

Keywords:

4-Aminothiophenol
 3-Aminopropyltriethoxysilane
 Graphene oxide
 Adsorption capacities

ABSTRACT

In this work, 4-aminothiophenol and 3-aminopropyltriethoxysilane were firstly used to functionalize graphene oxide (GO) in order to promote the sorption efficiencies of methylene blue (MB) and copper (Cu²⁺). Characterization experiments illustrated that sulfhydryl group (–SH) and amino group (–NH₂) were existed onto 4-aminothiophenol modified GO (GO-SH) and 3-aminopropyltriethoxysilane modified GO (GO-N), respectively. Adsorption isotherm results showed that the maximum adsorption capacities of MB by GO-SH and GO-N were 763.30 and 676.22 mg/g, which was much higher than original GO 455.95 mg/g. For Cu²⁺ adsorption, the maximum adsorption capacities by GO-SH and GO-N were 99.17 and 103.28 mg/g, suggesting that the engineered GO exhibited greater Cu²⁺ sorption ability than original GO 32.91 mg/g. Both MB and Cu²⁺ removal rates increased with pH and adsorbent dosage increased, while the sorption rates weakly reduced with increasing ionic strength. The modification by –SH and –NH₂ would not only increase the sorption sites, but also cause chelation with heavy metals, and thus improving the sorption capacities of MB and Cu²⁺.

© 2016 Elsevier B.V. All rights reserved.

* Corresponding author.

E-mail address: hywang96@126.com (H. Wang).

¹ These authors contributed equally to this work and should be considered co-first authors.

1. Introduction

With the rapid usage of dyes in industries such as paper, leather, rubber, textile, plastic, food, and dyestuffs [4,14], the release of MB in waste and underground water was intensively increased, which causes serious environmental problems such as cyanosis, quadriplegia, vomiting, diarrhea, and jaundice on human beings [10,18] and toxic to microorganisms. Hence, it is necessary to treat MB-containing wastewater before discharge.

Because Cu^{2+} is widely used in leather tanning, electroplating and mechanical manufacturing industry [27], a large amount of Cu^{2+} is appeared in surface and underground water, and thus resulting in vomit, convulsion, and even death on human beings [17]. In addition, it also bring about lots of adverse influences to natural environment due to that accumulated Cu^{2+} could not be easily removed and the enzyme activities of microorganisms are inhibited under excessive Cu^{2+} condition. Therefore, it is of great importance to eliminate the accumulated Cu^{2+} from wastewater before it is released to the surface waters.

Although there are many effective methods such as precipitation, membrane filtration, ion exchange [9], and aerobic or anaerobic treatment [20] to remove MB and Cu^{2+} , adsorption is the most widely used approach due to that it is insensitive to toxic pollutants [18], low cost and the experimental design is simple [19] for removing contaminations. Many studies have suggested sorbents such as carbon nanotubes, activated carbon [2], biochar [16], and montmorillonite [1], which are promising alternative methods for treatment of cationic dye and heavy metal ions.

Recently, graphene oxide has been considered as the most suitable adsorbent material for dye and heavy metal removal due to the reason that GO possesses high surface area [24], a variety of oxygen-containing functional groups and π -electron system [23], large numbers of reactive sites on nanosheet surface [15]. [22] prepared a nickel oxide/graphene oxide nanocomposite through hydrothermal method to remove MB from aqueous solution and the engineered GO shows much greater progress for removal of MB under visible light. Similarly, engineered GO coated with sand has been used as an adsorbent for the adsorption of Pb^{2+} and MB, and this material is efficient to remove dye and heavy metal [14]. In the study of Li and coworkers [20], the prepared calcium alginate immobilized GO is investigated to adsorb MB, and results show that the maximum adsorption capacity reaches 181.81 mg/g. Although graphene oxide performed effective adsorption capacities for dyes and heavy metals in some reports, it is also important to seek new and promising approaches for improving the treatment ability of GO.

In the present work, for the first time, two novel engineered GO nanocomposites were synthesized through graft modification with 4-aminothiophenol and 3-aminopropyltriethoxysilane for facilitating the removal processes of MB and Cu^{2+} from aqueous solutions. Because 4-aminothiophenol could supply functional groups ($-\text{SH}$) occurring chelation with heavy metals, the removal efficiency of heavy metal was enhanced [13]. Similarly, adsorption capacity would increase due to that functional groups ($-\text{NH}_2$) of 3-aminopropyltriethoxysilane often led to complexation with heavy metals [7]. A range of experiments were carried out to evaluate the adsorption abilities of the engineered GO to MB and Cu^{2+} in aqueous solutions. The objectives of this work were as follows: (a) prepare and characterize the engineered GO (GO-SH, GO-N); (b) evaluate the sorption capacity of MB and Cu^{2+} by GO-SH and GO-N; (c) investigate the effects of pH, dosage, and ionic strength on the adsorption process.

2. Materials and methods

2.1. Materials

All solutions used in this experiment were prepared using deionized water. All chemicals and reagents used in this experiment were guarantee reagents. In addition, 4-aminothiophenol ($\text{C}_6\text{H}_7\text{NS}$), 3-aminopropyltriethoxysilane ($\text{C}_9\text{H}_{23}\text{NO}_3\text{Si}$), hydrochloric acid (HCl), sodium hydroxide (NaOH), sulfuric acid (H_2SO_4), phosphoric acid (H_3PO_4), graphite powder, potassium permanganate (KMnO_4), hydrogen peroxide (H_2O_2), ethanol ($\text{C}_2\text{H}_6\text{O}$), sodium nitrite (NaNO_2), acetone (CH_3COCH_3), copper chloride ($\text{CuCl}_2 \cdot 2\text{H}_2\text{O}$), methylene blue (MB), sodium chloride (NaCl) were purchased from Aladdin and Qiangsong Fine Chemicals.

2.2. Engineered GO production

For preparation of GO, 720 mL H_2SO_4 and 80 mL H_3PO_4 was added to a three-necked flask, then 6.0 g graphite powder and 40 g KMnO_4 was slowly added to the mixture. After that, the reaction was stirred for 12 h under 50 °C condition. Afterwards, the reaction was heated to 90 °C for 2 h. When the mixture was cooled to room temperature, the mixture was poured onto 1000 mL ice. Next, 40% H_2O_2 was dropwise added to the mixture until brilliant yellow was appeared. The reacting solution was washed by 30% HCl (3 \times), ethanol (3 \times), and deionized water (9 \times). And then the mixture was vacuum-dried for 24 h under 50 °C condition. At last, 10 g GO was obtained.

For preparation of GO-SH, 5.0 g 4-aminothiophenol and 80 mL 1 M HCl was added to a three-necked flask, the temperature of the reaction was increased to 50 °C under stirring condition until 4-aminothiophenol was completely dissolved. Then, NaNO_2 solution (10 g NaNO_2 dissolved into 100 mL deionized water) was dropwise added to the reacting mixture under ice-bath condition until bubble was completely disappeared. After that, 5.0 g GO was dispersed in 200 mL deionized water and then added to the reacting solution. After 12 h stirring under ice-bath, the mixture was washed by acetone (3 \times), ethanol (3 \times), and deionized water (9 \times). At last, the mixture was vacuum-dried for 24 h under 50 °C condition, obtaining GO-SH.

For preparation of GO-N, 10 mL 3-aminopropyltriethoxysilane was added to 500 mL deionized water, and the solution was stirred for 5 h under 45 °C. Then the solution was centrifuged to obtain the supernatant. Afterwards, the supernatant was mixed with 0.5 mg/mL GO under stirring condition until tawny flocculent precipitates were appeared. After then, the flocculent precipitates were collected and washed by deionized water (9 \times). At last, the flocculent precipitates were vacuum-dried for 24 h under 50 °C condition, obtaining GO-N.

2.3. Engineered GO characterization

Surface morphology of the samples was determined using scanning electron microscopy (SEM) (ZEISS, Germany) equipped with an energy dispersive X-ray fluorescence spectroscopy EDS for analyzing surface elements. FTIR spectroscopy spectra of the samples were taken with a Nicolet 5700 spectrometer using KBr pellets in the range of 4000–400 cm^{-1} . XPS spectra were measured with a Thermo Fisher ESCALAB 250Xi. XRD spectra were obtained with an X-ray Diffractometer X'Pert Pro, PANalytical.

2.4. Adsorption kinetics and isotherm

In order to control quality, all the kinetic and isotherm experiments were conducted in duplicate and the differences of two measurements were lower than 3%.

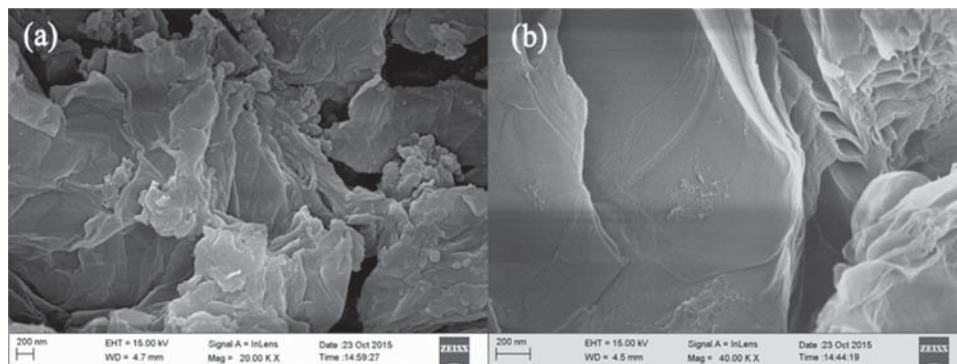


Fig. 1. SEM images of GO-SH (a) and GO-N (b).

Adsorption kinetics of MB and Cu^{2+} on the engineered GO were carried out by adding 0.01 and 0.05 g of each adsorbent to 200 mL Erlenmeyer flasks containing 100 mL MB and Cu^{2+} solution at 25 °C in a mechanical shaker. The initial concentrations of MB and Cu^{2+} were 60 mg/L and 40 mg/L. Samples were taken at 0, 2 min, 5 min, 10 min, 20 min, 50 min, 100 min, 150 min, 4 h, 8 h, 12 h, 24 h, 48 h, and filtered by 0.22 μm pore size microporous membrane, and then determined the MB and Cu^{2+} contents by Standard Method [3].

Adsorption isotherms of MB and Cu^{2+} on GO-SH and GO-N were conducted by adding 0.01 and 0.05 g of each adsorbent to 200 mL Erlenmeyer flasks containing 100 mL MB and Cu^{2+} solution at 25 °C in a mechanical shaker. The concentration of MB varied from 5 to 400 mg/L, while Cu^{2+} varied from 5 to 300 mg/L. After 24 h reaction, the samples were taken and determined the MB and Cu^{2+} contents by the same method.

2.5. Effects of pH, dosages, and ionic strength

The effect of pH was conducted by ranging solution pH (MB: 2–12, Cu^{2+} : 2–7) under dosage 0.01 g for MB sorption and 0.05 g for Cu^{2+} sorption. At pH of 6.0, the effect of dosage was carried out by adding 0.05, 0.1, 0.2, 0.3, 0.4 g/L engineered GO for MB sorption and 0.1, 0.3, 0.5, 0.7, 0.9 g/L engineered GO for Cu^{2+} sorption. For investigation of ionic strength, NaCl concentration was varied from 0 to 0.1 M. The initial concentrations of MB and Cu^{2+} were maintained at 80 mg/L and 60 mg/L, respectively.

3. Results and discussion

3.1. Physicochemical properties

The morphologies and nanostructures of GO-SH and GO-N were characterized by SEM technology. It is obvious that the surface of engineered GO represented wrinkling [20], aggregated nanosheets, and layered structure (Fig. 1). As shown in Fig. 2, large amounts of S were observed from the EDS spectrum of GO-SH, which demonstrated that 4-aminothiophenol was successfully grafted onto GO. When GO-SH adsorbed MB, the C, O contents changed. However, large numbers of Cu were observed after the Cu^{2+} sorption process and the C, O contents decreased, suggesting that copper ions were adsorbed onto GO-SH. For EDS spectrum of GO-N, the observed Si proved that 3-aminopropyltriethoxysilane was successfully grafted onto GO. There was an increase of C content after MB adsorption, while abundant Cu was detected after Cu^{2+} sorption, meaning that GO-N exhibited excellent MB and copper sorption abilities.

Fig. 3 illustrates the X-ray diffraction (XRD) patterns of GO-SH, GO-N, adsorbed GO-SH and GO-N. The obvious diffraction peak appeared at $2\theta \approx 10.00$ was attributing to the layer structure of GO [25]. For GO-SH, the diffraction peak was found at $2\theta \approx 17.20$, which

probably proved the presence of $-\text{SH}$. For GO-N, at $2\theta \approx 21.00$, the observed peak might correspond to the existence of $-\text{NH}_2$. When MB was adsorbed onto GO-SH and GO-N, the diffraction peaks at $2\theta \approx 10.00$ were decreased, which was due to the fact that MB replaced large numbers of adsorption sites on engineered GO. After Cu^{2+} adsorption, the XRD patterns of GO-SH and GO-N appeared lots of strong peaks at $2\theta \approx 16.21, 21.93, 23.72, 28.86, 33.98, 43.01, 47.43,$ and 57.38 , which was attributing to copper-containing compounds after adsorption onto engineered GO.

The FTIR spectra of engineered GO and adsorbed GO are shown in Fig. 4. For GO-SH, the vibration absorption peak of S-H was observed at 2233 cm^{-1} [5], suggesting that $-\text{SH}$ was grafted onto GO. However, this peak was disappeared after adsorbed MB and Cu^{2+} because MB and Cu^{2+} was integrated with $-\text{SH}$ functional groups during the adsorption process. Additionally, the peaks appeared at $1624, 1583, 1602\text{ cm}^{-1}$ of GO-SH, and adsorbed GO-SH were attributing to the bending vibrations of $\text{C}=\text{O}$. While, the C-O bonds caused peaks at $1070, 1078, 1091\text{ cm}^{-1}$, which demonstrated that the existence of numerous oxygen-containing functional groups. For GO-N, the characteristic peak appeared at 3402 cm^{-1} was attributing to the functional group $-\text{NH}_2$, which indicated the presence of amino groups in GO-N. However, after adsorbed MB and Cu^{2+} , this peak shifted to lower waves $3363,$ and 3361 cm^{-1} , which suggested that amino groups onto GO-N promoted the adsorption process. In addition, the obvious peaks of GO-N, GO-N-MB, GO-N-Cu appeared at $1631, 1598, 1595\text{ cm}^{-1}$ ($\text{C}=\text{O}$) and $1037, 1037, 1115\text{ cm}^{-1}$ ($\text{C}-\text{O}$), suggesting that the engineered GO possessed large numbers of oxygen-containing functional groups.

Fig. 5 shows the XPS spectra of engineered GOs and adsorbed engineered GOs. For GO-SH, the observed N and S elements demonstrated that $-\text{SH}$ was existed in GO. While for GO-N, N element was detected, suggesting the presence of $-\text{NH}_2$ on GO. After MB sorption, the peak of C spectrum was increased, indicating that MB was adsorbed onto engineered GO. The new peaks of Cu were observed of GO-SH and GO-N spectra after Cu^{2+} sorption, meaning that Cu was effectively adsorbed onto engineered GO.

3.2. Adsorption kinetics and isotherms

Adsorption kinetics of MB and Cu^{2+} by the engineered GO and original GO are shown in Fig. 6, while Table 1 illustrated the adsorption kinetics data of pseudo-first-order and pseudo-second-order models. For MB adsorption by GO-SH and GO-N, there was a fast initial phase in the first few hours and about 90% MB was removed during this phase. Then the removal rate was much slow to achieve equilibrium. For Cu^{2+} adsorption by GO-SH, 95% Cu^{2+} was adsorbed in the first few minutes, while the removal rate was relatively slow by GO-N. It is obvious that MB and Cu^{2+} adsorptions on GO-SH

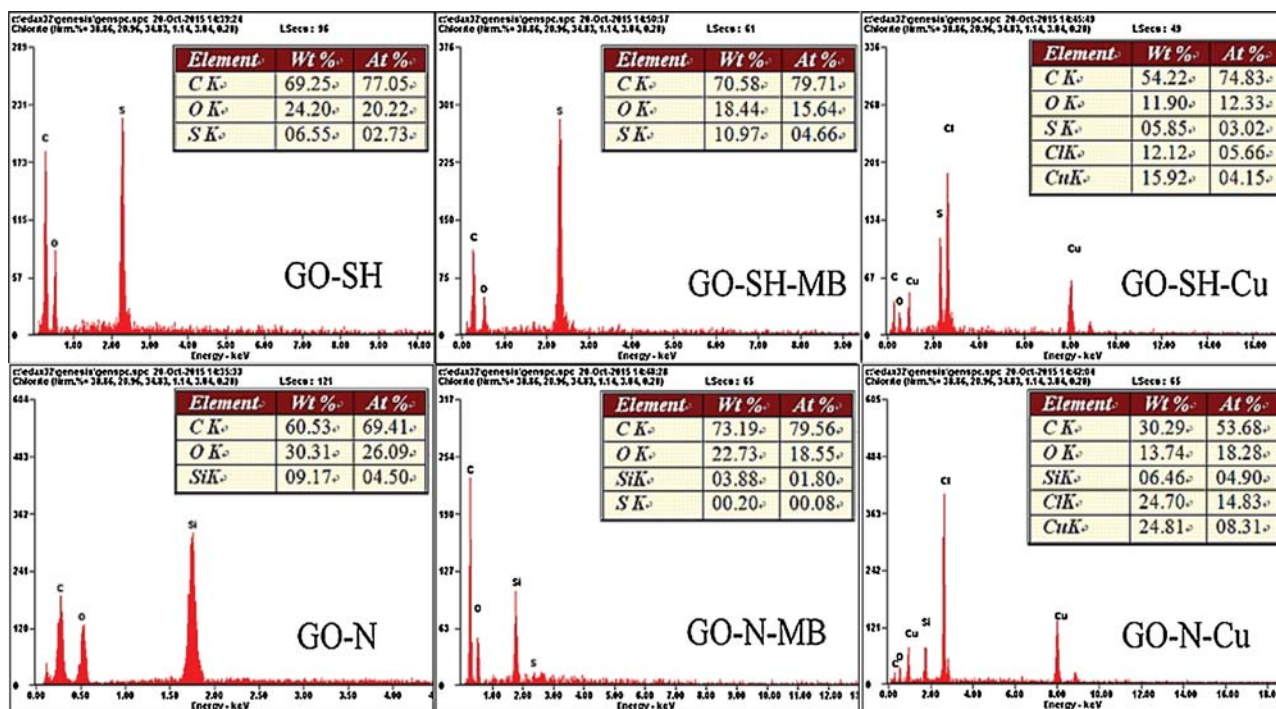


Fig. 2. EDS spectra of engineered GOs and adsorbed engineered GOs.

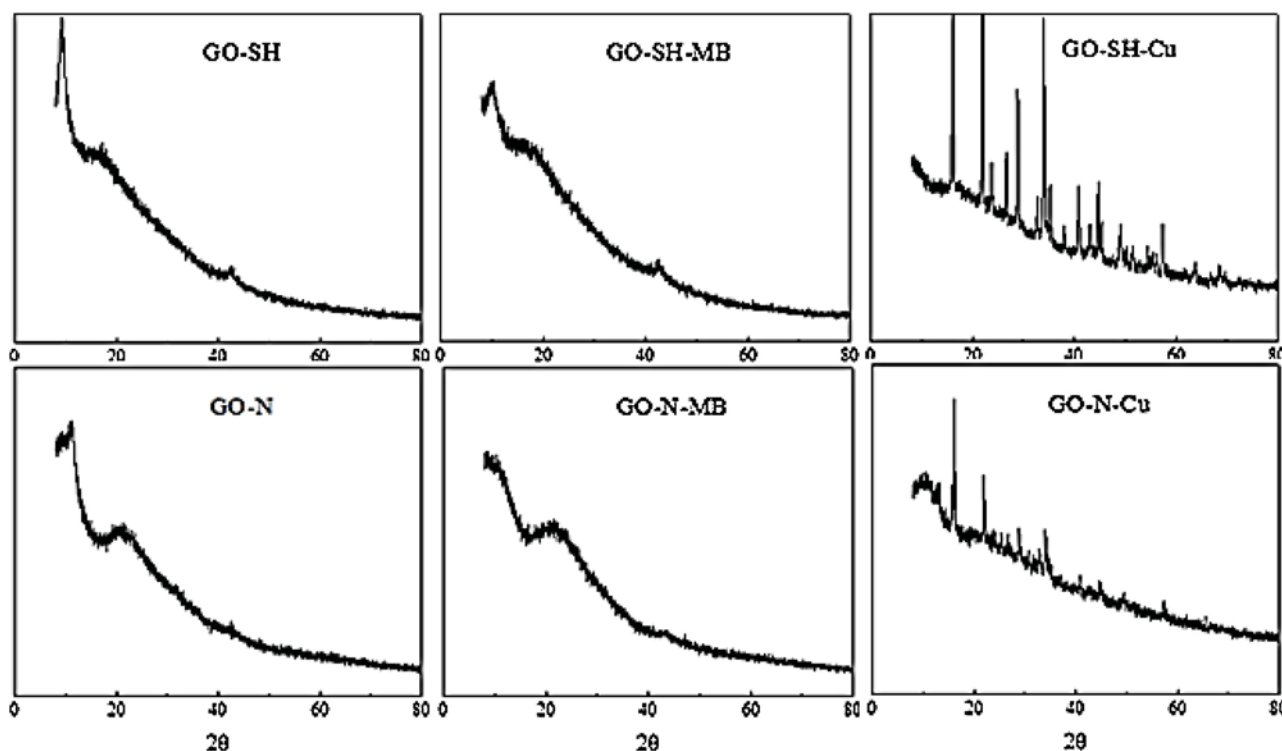


Fig. 3. XRD patterns of engineered GOs and adsorbed engineered GOs.

and GO-N were better fitted by the pseudo-second-order model than pseudo-first-order model (Table 1). For pseudo-second-order model, the adsorption rate constants k of engineered GO were higher than that of original GO, which showed that GO-SH and GO-N exhibited greater MB and Cu^{2+} sorption ability than GO.

MB and Cu^{2+} adsorption isotherms and adsorption isotherms data of Langmuir, Freundlich, Freundlich-Langmuir models by the

engineered GO and original GO are shown in Fig. 7 and Table 1, respectively. For MB adsorption, the data were better fitted by Langmuir model than Freundlich model, which demonstrated that the mainly adsorption types on GO-SH and GO-N were monolayer adsorption. The maximum adsorption capacity of MB by GO-SH was 763.30 mg/g, which was much higher than original GO 455.95 mg/g. In addition, GO-SH presented greater MB sorption ability than

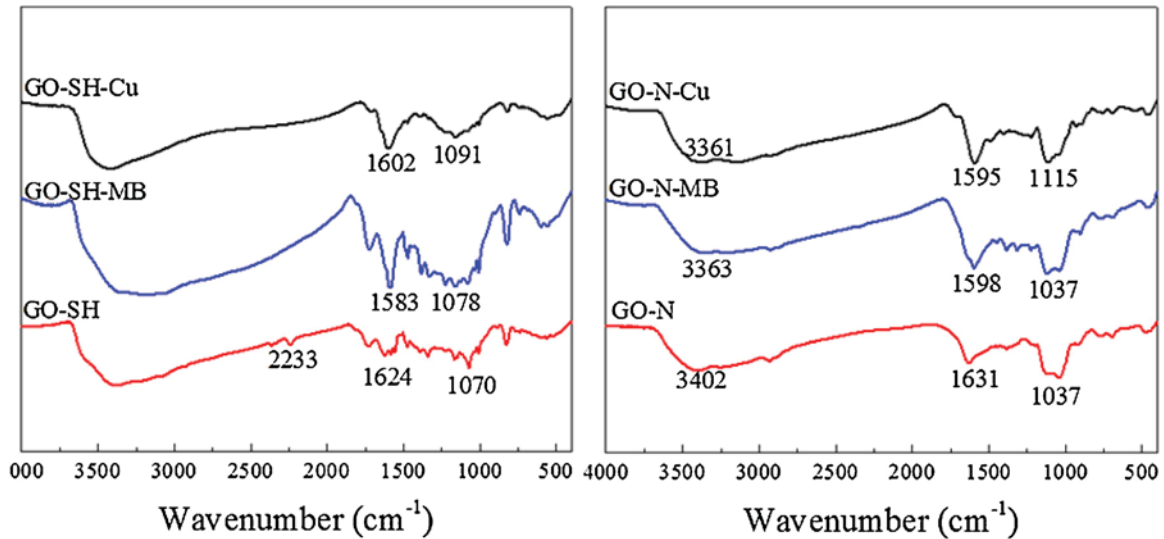


Fig. 4. FTIR spectra of engineered GOs and adsorbed engineered GOs.

Table 1
Best-fit parameters for kinetics and isotherm models of MB and Cu²⁺ sorption onto GO-SH and GO-N.

Equations		Parameter1	Parameter2	Parameter3	R ²
MB					
First-order	GO	$k_1 = 1.219$	$q_e = 414.900$		0.616
	GO-SH	$k_1 = 3.864$	$q_e = 558.100$		0.836
Second-order	GO	$k_2 = 0.181$	$q_e = 407.023$		0.983
	GO-SH	$k_2 = 1.377$	$q_e = 561.345$		0.978
Langmuir	GO	$K = 0.014$	$S_{max} = 455.950$		0.975
	GO-SH	$K = 0.020$	$S_{max} = 763.302$		0.988
Freundlich	GO	$K_f = 25.118$	$n = 0.483$		0.883
	GO-SH	$K_f = 48.827$	$n = 0.546$		0.905
Freundlich-Langmuir	GO	$K_r = 0.00008$	$S_{max} = 407.047$	$n = 2.486$	0.970
	GO-SH	$K_r = 0.0004$	$S_{max} = 550.890$	$n = 3.824$	0.966
MB					
First-order	GO	$k_1 = 1.219$	$q_e = 414.900$		0.616
	GO-N	$k_1 = 2.721$	$q_e = 528.104$		0.765
Second-order	GO	$k_2 = 0.181$	$q_e = 407.023$		0.983
	GO-N	$k_2 = 0.277$	$q_e = 521.645$		0.982
Langmuir	GO	$K = 0.014$	$S_{max} = 455.950$		0.975
	GO-N	$K = 0.028$	$S_{max} = 676.223$		0.981
Freundlich	GO	$K_f = 25.118$	$n = 0.483$		0.883
	GO-N	$K_f = 45.095$	$n = 0.557$		0.901
Freundlich-Langmuir	GO	$K_r = 0.00008$	$S_{max} = 407.047$	$n = 2.486$	0.970
	GO-N	$K_r = 0.0004$	$S_{max} = 512.736$	$n = 4.178$	0.960
Cu²⁺					
First-order	GO	$k_1 = 1.338$	$q_e = 32.100$		0.870
	GO-SH	$k_1 = 3.176$	$q_e = 87.030$		0.594
Second-order	GO	$k_2 = 0.145$	$q_e = 33.010$		0.890
	GO-SH	$k_2 = 0.249$	$q_e = 84.951$		0.802
Langmuir	GO	$K = 0.026$	$S_{max} = 32.910$		0.951
	GO-SH	$K = 0.122$	$S_{max} = 99.172$		0.935
Freundlich	GO	$K_f = 3.623$	$n = 0.305$		0.935
	GO-SH	$K_f = 7.823$	$n = 0.415$		0.942
Freundlich-Langmuir	GO	$K_r = 0.0002$	$S_{max} = 34.038$	$n = 1.986$	0.811
	GO-SH	$K_r = 0.0025$	$S_{max} = 98.390$	$n = 3.124$	0.915
Cu²⁺					
First-order	GO	$k_1 = 1.338$	$q_e = 32.100$		0.870
	GO-N	$k_1 = 2.297$	$q_e = 99.121$		0.709
Second-order	GO	$k_2 = 0.145$	$q_e = 33.010$		0.890
	GO-N	$k_2 = 0.238$	$q_e = 97.879$		0.958
Langmuir	GO	$K = 0.026$	$S_{max} = 32.910$		0.951
	GO-N	$K = 0.082$	$S_{max} = 103.281$		0.956
Freundlich	GO	$K_f = 3.623$	$n = 0.305$		0.935
	GO-N	$K_f = 10.724$	$n = 0.399$		0.958
Freundlich-Langmuir	GO	$K_r = 0.0002$	$S_{max} = 34.038$	$n = 1.986$	0.811
	GO-N	$K_r = 0.0021$	$S_{max} = 98.652$	$n = 2.923$	0.892

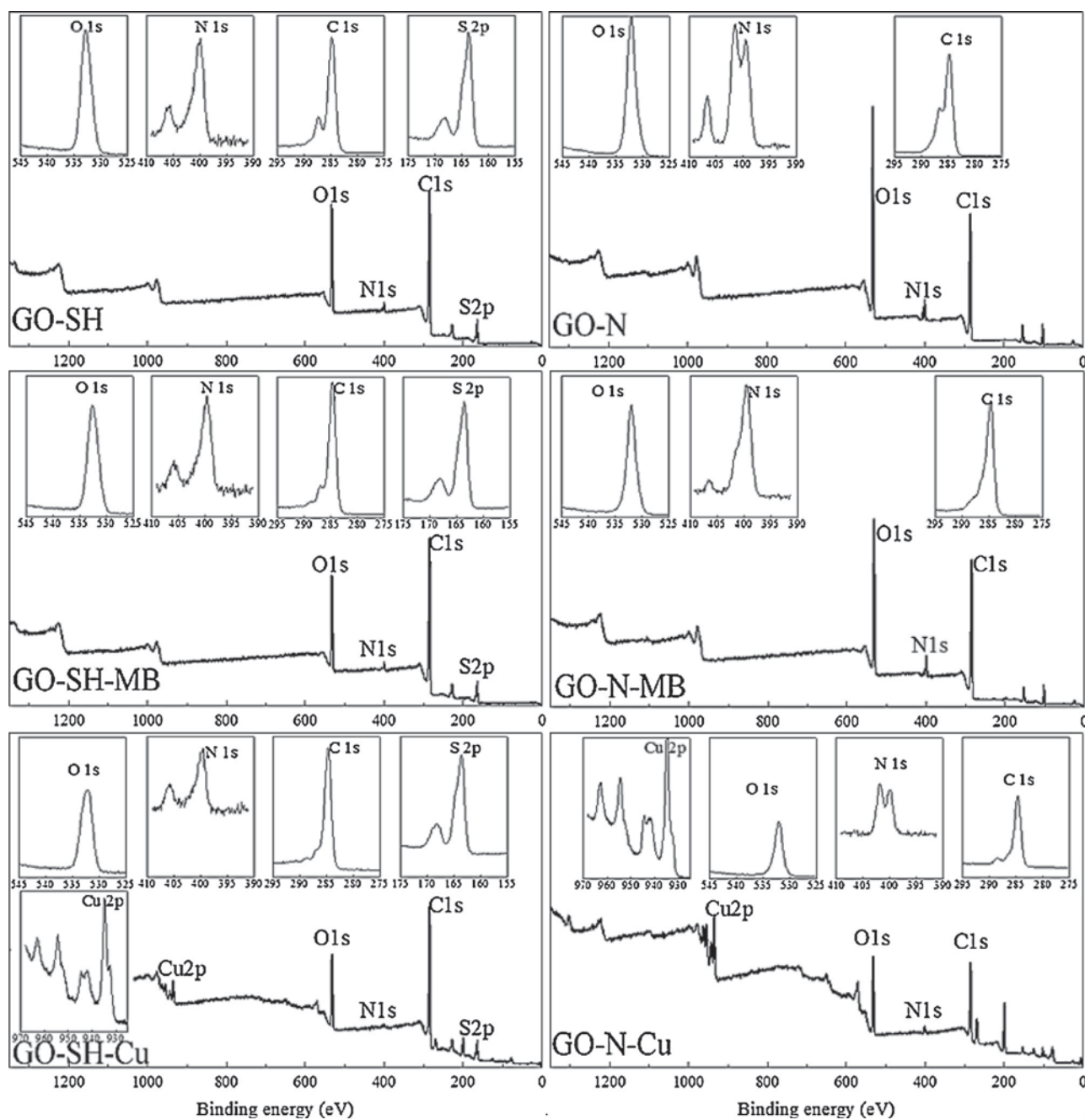


Fig. 5. XPS spectra of engineered GOs and adsorbed engineered GOs.

GO-N 676.22 mg/g. For Cu^{2+} adsorption, the maximum adsorption capacities by GO-SH and GO-N were 99.17 mg/g and 103.28 mg/g, respectively. Results showed that the adsorption isotherms data of Cu^{2+} were both well fitted by Langmuir model and Freundlich model, which illustrated that the adsorption of Cu^{2+} by GO-SH and GO-N might be controlled by multiple mechanisms. For Langmuir model, the maximum Cu^{2+} adsorption capacities by GO-SH and GO-N were 99.17 mg/g and 103.28 mg/g, which were much greater than original GO 32.91 mg/g. The adsorption isotherms results showed that the engineered GO exhibited greater MB and Cu^{2+} adsorption ability than original GO. The maximum sorption capacities of the engineered GO are greater than that of many other common sorbents reported in the literatures (Table 2), meaning that $-\text{SH}$ and $-\text{NH}_2$ modified GO can be considered as effective sorbents for MB and Cu^{2+} remediation.

Table 2

Maximum MB and Cu^{2+} sorption capacities of different sorbents.

	Adsorbent	Capacity(mg/g)	Reference
MB	GO	144.92	[20]
	GO/calcium alginate	181.81	[20]
	Carbon nanotubes	46.20	[29]
	GO	455.95	This study
	GO-SH	763.30	This study
Cu^{2+}	GO-N	676.22	This study
	CEMNPs	3.20	[6]
	GO aerogel	19.70	[21]
	GO	46.60	[28]
	Engineered biochar	34.20	[26]
	Chitosan-coated bentonite beads	12.20	[12]
	GO	32.91	This study
	GO-SH	99.17	This study
	GO-N	103.28	This study

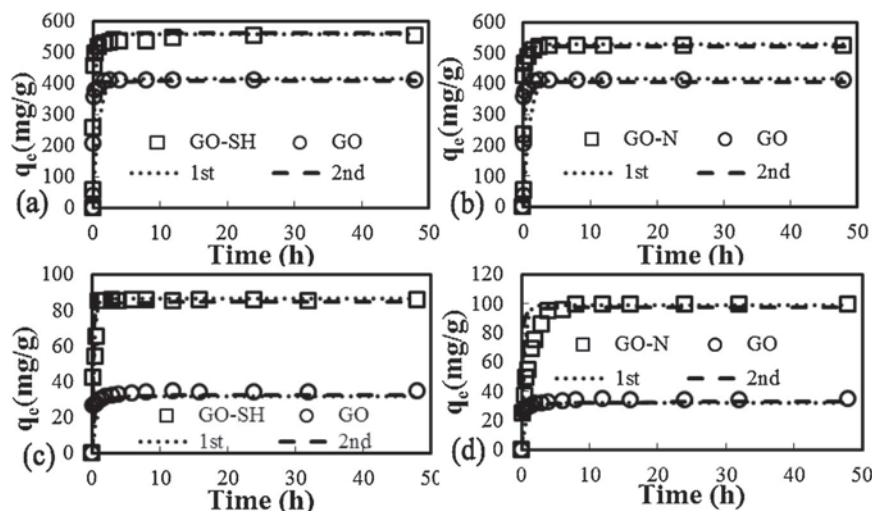


Fig. 6. Sorption kinetics: MB sorption kinetics data and fitted models for (a) GO and GO-SH, (b) GO and GO-N; Cu sorption kinetics data and fitted models for (c) GO and GO-SH, (d) GO and GO-N.

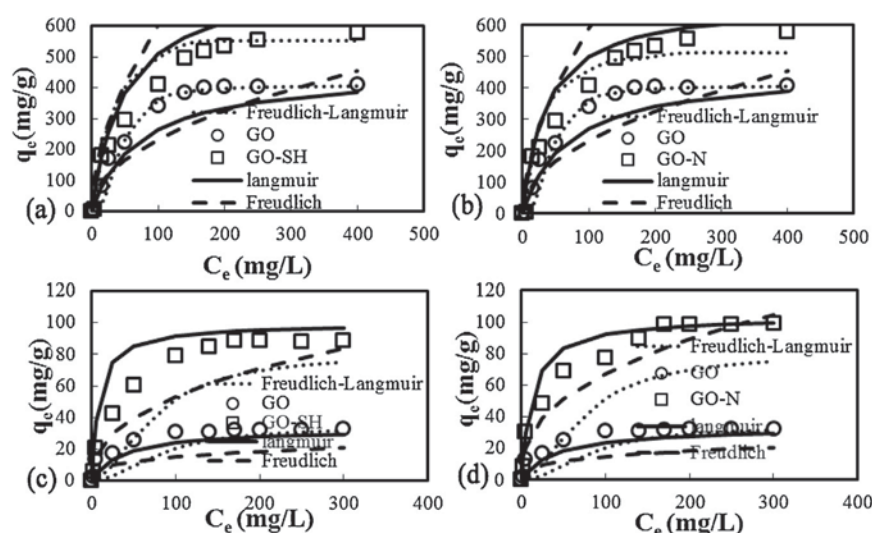


Fig. 7. Sorption isotherm: MB sorption isotherm data and fitted models for (a) GO and GO-SH, (b) GO and GO-N; Cu sorption isotherm data and fitted models for (c) GO and GO-SH, (d) GO and GO-N.

3.3. Effects of pH, dosages, and ionic strength

When pH increased, both the MB and Cu^{2+} removal rates increased (Fig. 8). For MB adsorption, the removal rates increased from 49.87% to 89.02% and 27.12% to 97.03% by GO-SH and GO-N with pH increased from 2 to 12. This phenomenon was attributed to that the surfaces of engineered GO were more negatively charged under alkaline environment, so that the cationic pigment (MB^+) could be easily adsorbed by GO-SH and GO-N through electrostatic forces [11,18]. For Cu^{2+} adsorption, when pH increased from 2 to 7, the removal rates increased from 19.05% to 95.93% and 21.11% to 97.02% by GO-SH and GO-N. The reason might be that the hydrogen ions would compete with Cu^{2+} for limited binding sites onto engineered GO at lower pH condition. However, the hydrogen ions decreased with pH increased so that Cu^{2+} had more opportunity to be adsorbed by engineered GO [25].

In general, the removal rates of MB and Cu^{2+} increased with increasing engineered GO dosage under constant initial MB and Cu^{2+} concentrations (Fig. 9). For MB adsorption, when the dosage of engineered GO increased from 0.05 to 0.40 g/L, the removal rates increased from 38.22% to 98.78% and 30.04% to 96.15% by GO-SH

and GO-N, respectively. Similarly, for Cu^{2+} adsorption by GO-SH and GO-N, the removal rates increased from 21.25% to 94.01 and 31.88% to 97.03% with engineered GO dose increased from 0.1 to 0.9 g/L. In addition, GO-SH performed better MB removal capacity than GO-N, while GO-N performed greater Cu^{2+} adsorption ability than GO-SH.

When ionic strength increased, MB and Cu^{2+} removal rates presented weakly decreases (Fig. 10). The removal rates of MB decreased from 76.20% to 65.87% and 61.12% to 58.01% by GO-SH and GO-N with ionic strength increased from 0 to 0.1 M, respectively. For Cu^{2+} removal, when ionic strength increased from 0 to 0.1 M, Cu^{2+} removal rates decreased from 75.17% to 67.32% and 85.02% to 66.98% by GO-SH and GO-N, respectively. The reason for this phenomenon might be that sodium ions would compete with MB^+ and Cu^{2+} for the limited adsorption sites onto engineered GO. On the other hand, the activity coefficients of MB^+ and Cu^{2+} would be influenced so that the sorption process would be inhibited [25]. Moreover, aggregation phenomenon was increased by increasing ionic strength and thus affecting the electrostatic interactions of sorption process [8].

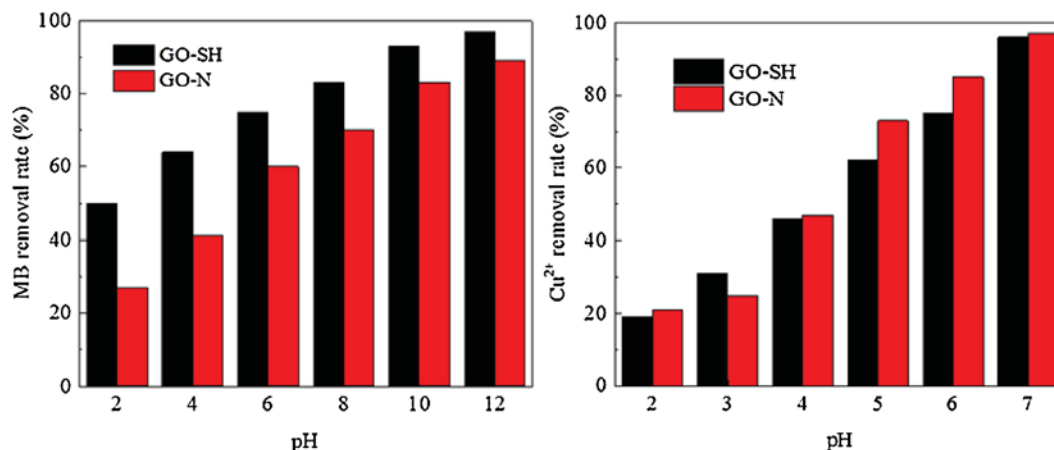


Fig. 8. Effect of pH on MB and Cu²⁺ adsorption by engineered GO.

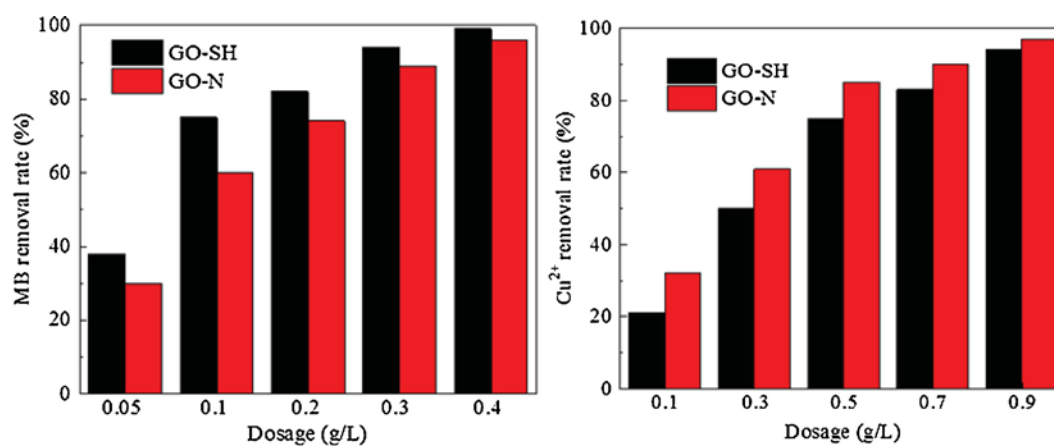


Fig. 9. Effect of dosage on MB and Cu²⁺ adsorption by engineered GO.

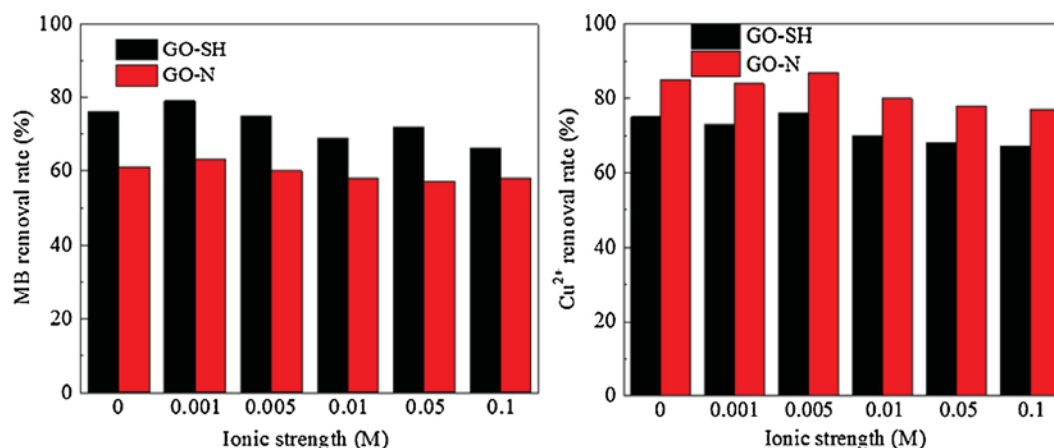


Fig. 10. Effect of ionic strength on MB and Cu²⁺ adsorption by engineered GO.

3.4. Adsorption mechanisms

The EDS and XPS spectra of GO-SH and GO-N showed evidences of the presence of 4-aminothiophenol and 3-aminopropyltriethoxysilane in engineered GO. In addition, FTIR spectra demonstrated that –SH and –NH₂ were really existed in GO-SH and GO-N, suggesting that –SH and –NH₂ were successfully grafted onto GO through grafting reaction. The results of sorption kinetics and isotherms showed that GO-SH and GO-N exhibited

much greater MB and Cu²⁺ adsorption capacities than original GO, indicating that the graft modification onto GO to promote MB and Cu²⁺ sorption was successful. For 4-aminothiophenol modified GO, abundant –SH could occur chelation with Cu²⁺, and thus improving Cu²⁺ removal efficiency. Moreover, more oxygen-containing functional groups would also enhance MB sorption. For GO-N, large amounts of –NH₂ could stretch over the layered structure of GO so that more sorption sites would bare for potential sorption. On the other hand, –NH₂ always formed

chelates with heavy metals, leading to greater adsorption ability of copper ions. Although GO could adsorb heavy metals and ions through electrostatic reaction or chemical adsorption because of its abundant epoxy group, carboxyl group, and hydroxyl group, the engineered GO (GO-SH and GO-N) showed much stronger binding affinity to MB and Cu^{2+} than original GO. In addition, this powder material could be separated from treated water by an external magnetic field through synthesizing magnetic GO nanoparticles.

4. Conclusions

Two novel engineered GO nanocomposites were synthesized through graft modification with 4-aminothiophenol and 3-aminopropyltriethoxysilane for MB and Cu^{2+} removal from aqueous solutions. This functionalization not only increased the sorption sites for potential MB and Cu^{2+} removal, but also formed chelates with copper ions. As a result, the engineered GO showed much greater MB and Cu^{2+} sorption capacities than original GO. This functionalization approach thus could be considered as an effective method to synthesize engineered GO sorbents for dye and heavy metal removal.

Acknowledgments

This work was financially supported by the National Natural Science Foundation of China (NSFC) (51378400) and the National Science and Technology Pillar Program (2014BAL04B04).

References

- [1] C.A.P. Almeida, N.A. Debacher, A.J. Downs, L. Cottet, C.A.D. Mello, Removal of methylene blue from colored effluents by adsorption on montmorillonite clay, *J. Colloid Interface Sci.* 332 (1) (2009) 46–53.
- [2] S. Altenor, B. Carene, E. Emmanuel, J. Lambert, J.J. Ehrhardt, S. Gaspard, Adsorption studies of methylene blue and phenol onto vetiver roots activated carbon prepared by chemical activation, *J. Hazard. Mater.* 165 (1–3) (2009) 1029–1039.
- [3] Apha, Standard Methods for the Examination of Water and Wastewater, American Public Health Association, 2005.
- [4] N. Atar, A. Olgun, S.B. Wang, S.M. Liu, Adsorption of anionic dyes on boron industry waste in single and binary solutions using batch and fixed-bed systems, *J. Chem. Eng. Data* 56 (3) (2011) 508–516.
- [5] F. Beckert, C. Friedrich, R. Thomann, R. Mulhaupt, Sulfur-functionalized graphenes as macro-chain-transfer and RAFT agents for producing graphene polymer brushes and polystyrene nanocomposites, *Macromolecules* 45 (17) (2012) 7083–7090.
- [6] M. Bystrzejewski, K. Pyrzynska, A. Huczko, H. Lange, Carbon-encapsulated magnetic nanoparticles as separable and mobile sorbents of heavy metal ions from aqueous solutions, *Carbon* 47 (4) (2009) 1201–1204.
- [7] S.E. Cabaniss, Forward modeling of metal complexation by NOM: II. Prediction of binding site properties, *Environ. Sci. Technol.* 45 (8) (2011) 3202–3209.
- [8] W.H. Casey, Chemistry of the solid water interface—processes at the mineral water and particle water interface in natural systems—Stumm, W, *Nature* 363 (6426) (1993), 222–222.
- [9] J.H. Chen, H.T. Xing, X. Sun, Z.B. Su, Y.H. Huang, W. Weng, S.R. Hu, H.X. Guo, W.B. Wu, Y.S. He, Highly effective removal of Cu(II) by triethylenetetramine-magnetic reduced graphene oxide composite, *Appl. Surf. Sci.* 356 (2015) 355–363.
- [10] L.H. Chen, A. Ramadan, L.L. Lu, W.J. Shao, F. Luo, J. Chen, Biosorption of methylene blue from aqueous solution using lawn grass modified with citric acid, *J. Chem. Eng. Data* 56 (8) (2011) 3392–3399.
- [11] L. Cui, X. Guo, Q. Wei, Y. Wang, L. Gao, L. Yan, T. Yan, B. Du, Removal of mercury and methylene blue from aqueous solution by xanthate functionalized magnetic graphene oxide: sorption kinetic and uptake mechanism, *J. Colloid Interface Sci.* 439 (2015) 112–120.
- [12] M.L.P. Dalida, A.F.V. Mariano, C.M. Futralan, C.C. Kan, W.C. Tsai, M.W. Wan, Adsorptive removal of Cu(II) from aqueous solutions using non-crosslinked and crosslinked chitosan-coated bentonite beads, *Desalination* 275 (1–3) (2011) 154–159.
- [13] W. Gao, M. Majumder, L.B. Alemany, T.N. Narayanan, M.A. Ibarra, B.K. Pradhan, P.M. Ajayan, Engineered graphite oxide materials for application in water purification, *ACS Appl. Mater. Interfaces* 3 (6) (2011) 1821–1826.
- [14] J.L. Gong, Y.L. Zhang, Y. Jiang, G.M. Zeng, Z.H. Cui, K. Liu, C.H. Deng, Q.Y. Niu, J.H. Deng, S.Y. Huan, Continuous adsorption of Pb(II) and methylene blue by engineered graphene oxide coated sand in fixed-bed column, *Appl. Surf. Sci.* 330 (2015) 148–157.
- [15] J.Y. Huang, Z.W. Wu, L.W. Chen, Y.B. Sun, Surface complexation modeling of adsorption of Cd(II) on graphene oxides, *J. Mol. Liq.* 209 (2015) 753–758.
- [16] M. Inyang, B. Gao, Y. Yao, Y.W. Xue, A.R. Zimmerman, P. Pullammanappallil, X.D. Cao, Removal of heavy metals from aqueous solution by biochars derived from anaerobically digested biomass, *Bioresour. Technol.* 110 (2012) 50–56.
- [17] X. Li, X.P. Tang, Y.F. Fang, Using graphene oxide as a superior adsorbent for the highly efficient immobilization of Cu(II) from aqueous solution, *J. Mol. Liq.* 199 (2014) 237–243.
- [18] Y.H. Li, Q.J. Du, T.H. Liu, X.J. Peng, J.J. Wang, J.K. Sun, Y.H. Wang, S.L. Wu, Z.H. Wang, Y.Z. Xia, L.H. Xia, Comparative study of methylene blue dye adsorption onto activated carbon, graphene oxide, and carbon nanotubes, *Chem. Eng. Res. Des.* 91 (2) (2013) 361–368.
- [19] Y.H. Li, Q.J. Du, T.H. Liu, Y. Qi, P. Zhang, Z.H. Wang, Y.Z. Xia, Preparation of activated carbon from *Enteromorpha prolifera* and its use on cationic red X-GRL removal, *Appl. Surf. Sci.* 257 (24) (2011) 10621–10627.
- [20] Y.H. Li, Q.J. Du, T.H. Liu, J.K. Sun, Y.H. Wang, S.L. Wu, Z.H. Wang, Y.Z. Xia, L.H. Xia, Methylene blue adsorption on graphene oxide/calcium alginate composites, *Carbohydr. Polym.* 95 (1) (2013) 501–507.
- [21] X. Mi, G.B. Huang, W.S. Xie, W. Wang, Y. Liu, J.P. Gao, Preparation of graphene oxide aerogel and its adsorption for Cu^{2+} ions, *Carbon* 50 (13) (2012) 4856–4864.
- [22] X.S. Rong, F.X. Qiu, C. Zhang, L. Fu, Y.Y. Wang, D.Y. Yang, Adsorption-photodegradation synergetic removal of methylene blue from aqueous solution by NiO/graphene oxide nanocomposite, *Powder Technol.* 275 (2015) 322–328.
- [23] V. Singh, D. Joung, L. Zhai, S. Das, S.I. Khondaker, S. Seal, Graphene based materials: past, present and future, *Prog. Mater. Sci.* 56 (8) (2011) 1178–1271.
- [24] S. Stankovich, D.A. Dikin, G.H. Dommett, K.M. Kohlhaas, E.J. Zimney, E.A. Stach, R.D. Piner, S.T. Nguyen, R.S. Ruoff, Graphene-based composite materials, *Nature* 442 (7100) (2006) 282–286.
- [25] P. Tan, J. Sun, Y.Y. Hu, Z. Fang, Q. Bi, Y.C. Chen, J.H. Cheng, Adsorption of Cu^{2+} , Cd^{2+} and Ni^{2+} from aqueous single metal solutions on graphene oxide membranes, *J. Hazard. Mater.* 297 (2015) 251–260.
- [26] H. Wang, B. Gao, S. Wang, J. Fang, Y. Xue, K. Yang, Removal of Pb(II) Cu(II), and Cd(II) from aqueous solutions by biochar derived from KMnO_4 treated hickory wood, *Bioresour. Technol.* 197 (2015) 356–362.
- [27] H.T. Xing, J.H. Chen, X. Sun, Y.H. Huang, Z.B. Su, S.R. Hu, W. Weng, S.X. Li, H.X. Guo, W.B. Wu, Y.S. He, F.M. Li, Y. Huang, NH_2 -rich polymer/graphene oxide use as a novel adsorbent for removal of Cu(II) from aqueous solution, *Chem. Eng. J.* 263 (2015) 280–289.
- [28] S.T. Yang, Y. Chang, H. Wang, G. Liu, S. Chen, Y. Wang, Y. Liu, A. Cao, Folding/aggregation of graphene oxide and its application in Cu^{2+} removal, *J. Colloid Interface Sci.* 351 (1) (2010) 122–127.
- [29] Y. Yao, F. Xu, M. Chen, Z. Xu, Z. Zhu, Adsorption behavior of methylene blue on carbon nanotubes, *Bioresour. Technol.* 101 (9) (2010) 3040–3046.